Proceedings of the
Annual Stability Conference
Structural Stability Research Council
Baltimore, Maryland, April 10-13, 2018

Computational Study of Tension Field Action in Gable Frame Panel Zones

Gengrui Wei[1], Ioannis Koutromanos[2], Thomas M. Murray[3], Matthew R. Eatherton[4]

Abstract
Gable metal frames are popular, cost-efficient structural systems for commercial and industrial buildings. The use of relatively thin web material typically leads to buckling of the panel zone in the beam-to-column connections when the frame is subjected to lateral loads. However, the panel zones may still be capable of developing post-buckling resistance by means of tension field action (TFA). Previous experimental research has shown that the exterior corner of a panel zone in gable frame knee joints may not be stiff enough to fully develop TFA. Although these test results have demonstrated the development of post-buckling strength, the amount of TFA and the design parameters that affect such action are not well understood. This paper presents a theoretical model for TFA in knee joints based on plastic analysis, and an accompanying equation for predicting the post-buckling panel zone strength for positive bending (wherein the tension field is oriented from the interior to the exterior corners). The TFA was found to primarily depend on three design parameters, namely, flange flexural strength, panel aspect ratio, and panel slenderness. To calibrate the proposed equation, a parametric analytical study was conducted using the finite element method. The modeling scheme accounted for material and geometric nonlinearity and was validated with experimental test data. The study involved 98 prototype gable frame configurations and allowed the investigation of the impact of the aforementioned three design parameters on the TFA. The proposed equation was found to predict the panel zone shear strength for the prototype frames with an average error of 1% and an error standard deviation of 5%. Therefore, the equation can be used to calculate the post-buckling shear strength of panel zones for the range of design parameters considered in the parametric study.

1. Introduction
Metal building systems are popular for low-rise buildings because they are associated with fast construction and cost efficiency. The corner regions of a gable frame in metal building systems are sometimes referred to as knee joints and the column web in the knee joint is the panel zone. As the knee joint undergoes bending, the panel zone is subjected to significant shear force.

[1] Graduate Research Assistant, Virginia Tech, <gwei1@vt.edu>
[2] Assistant Professor, Virginia Tech, <ikoutrom@vt.edu>
[3] Emeritus Professor, Virginia Tech, <thmurray@vt.edu>
[4] Associate Professor, Virginia Tech, <meather@vt.edu>

Experimental tests by Young and Murray (1997) have demonstrated that knee joints subjected to positive bending (tension on the bottom flange of the rafter) can develop some post-shear-buckling resistance due to tension field action (TFA). In Table 1, the experimental shear strength of the panel zone in test specimens is compared to the nominal shear strength calculated with AISC 360-16 Eq. G2-7 (AISC 2016) with and without the consideration of full tension field action. It can be observed that the shear strength of all specimens exceeded the value V_{cr} corresponding to shear buckling, but was less than the sum, $V_{cr} + V_{TFA}$, corresponding to full TFA. Therefore, TFA was partially developed in these test specimens.

The tests by Young and Murray (1997) were conducted on a limited number of specimens, and could not allow a reliable estimation of the amount of TFA that can be developed for a knee joint. For this reason, the AISC Design Guide 16 (Murray and Shoemaker 2002) does not allow the consideration of TFA in shear design of knee joint panel zones subjected to positive bending.

To make use of the post-buckling shear strength for a more efficient and economical design, it is beneficial to study the amount of TFA, the consistency of the level of action, and the design parameters that affect the action in this type of structures. This paper describes an analytical and computational study that investigates the shear strength of thin panel zones in knee joints subjected to positive bending. A theoretical model was created to derive prediction equations for the strength, and a parametric study with finite element analyses was conducted to validate these proposed equations.

Table 1 Shear strength of knee joint specimens in Young and Murray (1997)

Specimen #	1	2	3	4
V_{exp} (kips)	43.2	46.8	119	148
V_{exp} / V_{cr}	1.18	1.48	2.33	3.68
$V_{exp} / (V_{cr} + V_{TFA})$	0.64	0.64	0.67	0.77

Note: V_{exp} = shear strength obtained from the experiments;
V_{cr} = shear buckling strength of web panel;
V_{TFA} = shear strength developed by tension field action

2. Theoretical Model for TFA in Knee Joints under Positive Bending

A theoretical model is established based on plastic analysis to predict the post-buckling shear strength of a knee joint panel zone subjected to positive bending. The model is based on the following assumptions:

1) The panel zone web plate is simply supported along its four edges by the panel zone flanges. This assumption is similar to that by Porter et al. (1975).
2) The panel zone flanges develop plastic hinges at the exterior corner of the panel zone. These hinges lead to a mechanism in the panel zone after it buckles (see Rockey 1971, Porter et al. 1975).
3) The tensile stress in the tension field is uniformly distributed and its orientation is aligned with the diagonal of the panel plate (Rockey 1971).
4) The two panel edges on the rafter and column sides are rigid in-plane, but can undergo rigid body rotation relative to one another.
5) The shear capacity associated with buckling V_{cr} remains constant after the panel buckles (Porter et al. 1975).

The shear strength, V_{PZ}, of the panel zone considering the contribution of TFA is given by:

$$V_{PZ} = V_{cr} + V_{TFA} \tag{1}$$

The shear buckling strength, V_{cr}, is given by:

$$V_{cr} = A_v \tau_{cr} = d_c t_w \tau_{cr} \tag{2}$$

where A_v is the overall area of the panel web plate cross section along the top of column, d_c is the full depth of the panel zone along the top of column, t_w is the thickness of the panel web plate, and τ_{cr} is the critical shear stress at buckling. For a simply supported rectangular plate, τ_{cr} is given by (Timoshenko and Gere 1961):

$$\tau_{cr} = K\left[\frac{\pi^2 E}{12\left(1-\mu^2\right)}\right]\left(\frac{t_w}{h_c}\right)^2 \tag{3}$$

where K is a buckling coefficient. The value of K is given by the following expression (Ziemian 2010):

$$K = \begin{cases} 5.34 + 4\left(\dfrac{h_c}{h_r}\right)^2 & \text{for } \dfrac{h_c}{h_r} < 1.0 \\ 5.34\left(\dfrac{h_c}{h_r}\right)^2 + 4 & \text{for } \dfrac{h_c}{h_r} > 1.0 \end{cases} \tag{4}$$

Parameters h_c and h_r in Eq. 4 correspond to the panel width (column web height) and panel height (rafter web height), respectively.

For an infinitesimal square element in the tension field of panel zone, the stress tensor can be transformed into a coordinate system aligned with the direction of the tension field (Fig. 1a). At the ultimate state, the transformed stress components must satisfy the Von Mises yield criterion:

$$\sqrt{\sigma_\xi^2 + \sigma_\eta^2 - \sigma_\zeta \sigma_\eta + 3\tau^2} = \sigma_{yw} \tag{5a}$$

where σ_{yw} is the yield stress of the web plate.

One can obtain the following expression for the diagonal tension field stress when the plate yields:

$$\sigma_t^y = -\frac{3}{2}\tau_{cr}\, sin\, 2\theta + \sqrt{\sigma_{yw}^2 + \tau_{cr}^2\left(\left(\frac{3}{2} sin\, 2\theta\right)^2 - 3\right)} \tag{5b}$$

where θ is the angle between the panel web diagonal and the horizontal face of the panel zone.

Fig. 1b schematically summarizes the assumed plastic mechanism for a knee joint panel zone subjected to shear force. Plastic hinges develop in the exterior flanges at distances c_1 and c_2 from the external corner of the panel, as also shown in Fig. 1b. The values of c_1 and c_2 can be obtained by considering equilibrium of the flange segments XY and XZ and given as follows:

$$c_1 = \frac{1}{sin\theta}\sqrt{\frac{2\left(M_{P1}+M_{P,min}\right)}{\sigma_t^y t_w}} \tag{6}$$

$$c_2 = \frac{1}{cos\theta}\sqrt{\frac{2\left(M_{P2}+M_{P,min}\right)}{\sigma_t^y t_w}} \tag{7}$$

where $M_{P1} = \frac{\sigma_{yf} b_{f1} t_{f1}^2}{4}$, $M_{P2} = \frac{\sigma_{yf} b_{f2} t_{f2}^2}{4}$ are the plastic moment capacity values of the flange sections and $M_{P,min} = min\left(M_{P1}, M_{P2}\right)$.

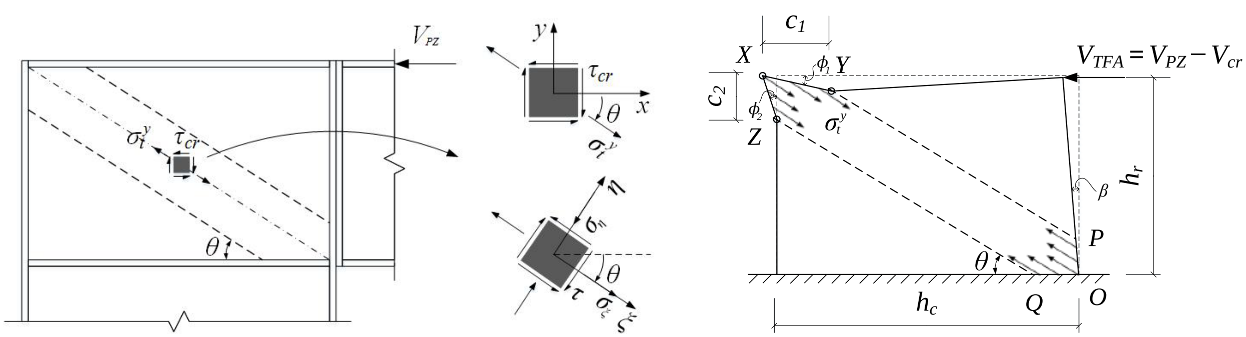

(a) Stress transformation of an element on the diagonal of panel zone

(b) Proposed failure mechanism with virtual displacements

Figure 1: Panel zone subjected to pure shear

The tension field strength, V_{TFA}, corresponding to the assumed mechanism can be obtained by employing the principle of virtual work for the mechanism:

$$W_{ext} = W_{int} \tag{8}$$

where W_{ext} and W_{int} are the virtual external work and virtual internal work, respectively. The values of the two virtual work quantities can be obtained by the following equations.

$$\begin{aligned} W_{ext} = {} & V_{TFA}\left(c_2\phi_2\right) - \sigma_t^y t_w\left(c_1 \, sin\theta\right) cos\theta \cdot c_2\phi_2 + \sigma_t^y t_w\left(c_1 \, sin\theta\right) sin\theta \cdot \frac{1}{2}c_1\phi_1 \\ & - \sigma_t^y t_w\left(c_2 \, cos\theta\right) cos\theta \cdot \frac{1}{2}c_2\phi_2 + \sigma_t^y t_w\left(c_2 \, cos\theta\right) cos\theta \cdot \frac{1}{2}c_2\beta \end{aligned} \tag{9a}$$

$$W_{int} = M_{P,min}\left(\phi_1+\phi_2\right) + M_{P1}\left(\phi_1+\beta\right) + M_{P2}\phi_2 \tag{9b}$$

where

$$\begin{aligned} c_1\phi_1 &= \left(h_c - c_1\right)\beta \\ c_2\phi_2 &= h_r\beta \end{aligned} \tag{10}$$

Solving equation $W_{ext} = W_{int}$ for V_{TFA} results in:

$$V_{TFA} = \frac{M_{P1} - M_{P2} - M_{P,min}}{h_r} + cos\,\theta\sqrt{2\sigma_t^y t_w}\left(\sqrt{M_{P1} + M_{P,min}} + \sqrt{M_{P2} + M_{P,min}}\right) \tag{11}$$

The critical shear stress can be expressed as $\tau_{cr} = C_v \tau_y$, where $\tau_y = \dfrac{\sigma_{yw}}{\sqrt{3}}$ and

$$C_v = \sqrt{3}K\left[\frac{\pi^2\, E/\sigma_{yw}}{12\left(1-\mu^2\right)}\right]\left(\frac{t_w}{h_c}\right)^2 \tag{12}$$

Eq. 5b can also be written as:

$$\sigma_t^y = C_t \sigma_{yw} \tag{13}$$

where

$$C_t = -\frac{\sqrt{3}C_v h_c h_r}{h_c^2 + h_r^2} + \sqrt{1 + \frac{C_v^2}{3}\left(\left(\frac{3h_c h_r}{h_c^2 + h_r^2}\right)^2 - 3\right)} \tag{14}$$

If one defines the dimensionless ratios $M_{P1}^* = \dfrac{M_{P1}}{M_y}$ and $M_{P2}^* = \dfrac{M_{P2}}{M_y}$, where $M_y = \dfrac{t_w h_c^2 \sigma_{yw}}{6}$, Eq. 11 can be written as:

$$V_{TFA} = \left[\frac{M_{P1}^* - M_{P2}^* - M_{P,min}^*}{6\,tan\,\theta} + cos\,\theta\sqrt{\frac{C_t}{3}}\left(\sqrt{M_{P1}^* + M_{P,min}^*} + \sqrt{M_{P2}^* + M_{P,min}^*}\right)\right]h_c t_w \sigma_{yw} \tag{15}$$

Section 4 of this paper will discuss a modification to Eq. 15 that adjusts for actual boundary conditions and the final equations are included in the Conclusion section.

3. Finite Element Modeling Approach and Validation

A computational study is performed using the commercial finite element program *LS-DYNA* (LSTC 2016a; LSTC 2016b), which is capable of simulating structural response in the presence of material nonlinearity, large displacements and large strains. The models of the prototype structures employ shell elements with selectively reduced integration, using the formulation of Hughes and Liu (1981), to capture the inelastic hysteretic material behavior and the buckling of panel regions. As shown in Fig. 2, refined three-dimensional shell element assemblages simulate the connection regions, while the remainder of the frame members are modeled with much simpler frame (beam) elements, as this remainder of the frame is assumed to remain elastic during the loading and its behavior is not of primary interest in this study. The kinematics of the beam elements are also governed by the formulation of Hughes and Liu (1981).

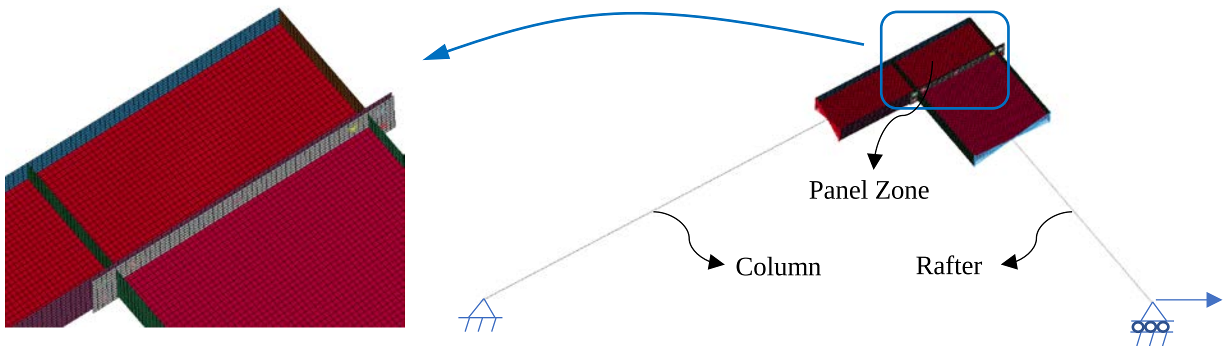

Figure 2: Finite element model with high-fidelity representation of the connection regions

The model shown in Fig. 2 simulates a knee joint subjected to positive bending. The end of the beam (at the approximate inflection point of the portal frame) and bottom of column are assumed to be points of zero moment. The application of loads as shown in Fig. 2 produces combinations of member axial force and bending moment which are consistent with those in a real building. Based on a mesh sensitivity study, an element size of 0.5 in. for the shell elements was found to lead to practically converged results in terms of load-deformation response and deformation patterns. An initial imperfection was also introduced in the original geometry of each mesh based on the first buckling mode such that the maximum initial out-of-plane deviation of the panel web is 1/72 times the maximum in-plane panel plate dimension. The specific value equals the tolerance allowed for deviations from a plane in the webs of built-up plate girders according to MBMA (MBMA 2012). An elastoplastic constitutive model, using a von Mises yield surface, linear kinematic hardening, and an associative flow rule was used to model the steel. The modulus of elasticity and hardening modulus were set equal to 29,000 ksi and 400 ksi, respectively.

To validate the finite element modeling approach for this study, two specimens tested by Young and Murray (1997) were simulated, to ensure that the computational models can satisfactorily capture the experimentally observed load-displacement response and buckling modes. The analytically obtained force-displacement curves for the two specimens are compared to the corresponding test results in Fig. 3. The peak force values obtained from the experiments and the FEA are 16.9 kips and 18.5 kips, respectively, for the first specimen. The peak force values for the second specimen are 21.9 kips and 23.6 kips, respectively. The discrepancy between the analytically obtained and experimentally recorded peak force values is most likely due to the existence of residual stress in the panel zone and surrounding flanges. Such residual stresses are not accounted for in the computational models. Fig. 4 shows the deformed shapes of the specimens in the tests and the simulations. Overall, the FEA results agree reasonably well with the test data.

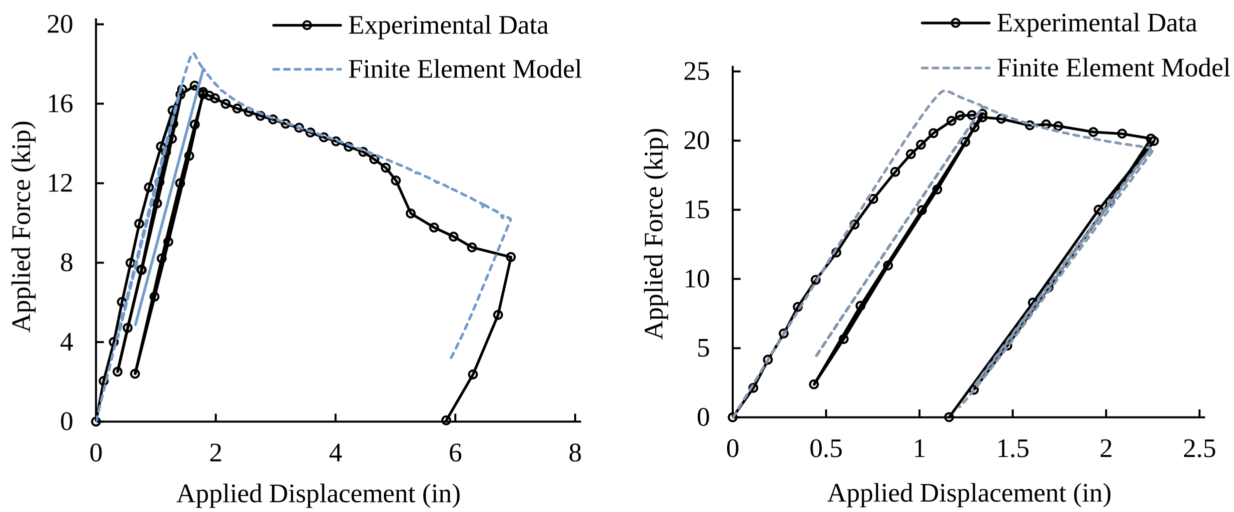

(a) Specimen 1 (b) Specimen 2

Figure 3: Force-displacement response for validation analyses of specimens tested by Young and Murray (1997)

Figure 4a: Comparison of analytically obtained and experimentally observed deformation patterns, for validation analyses of the knee joint Specimen 1 tested by Young and Murray (1997)

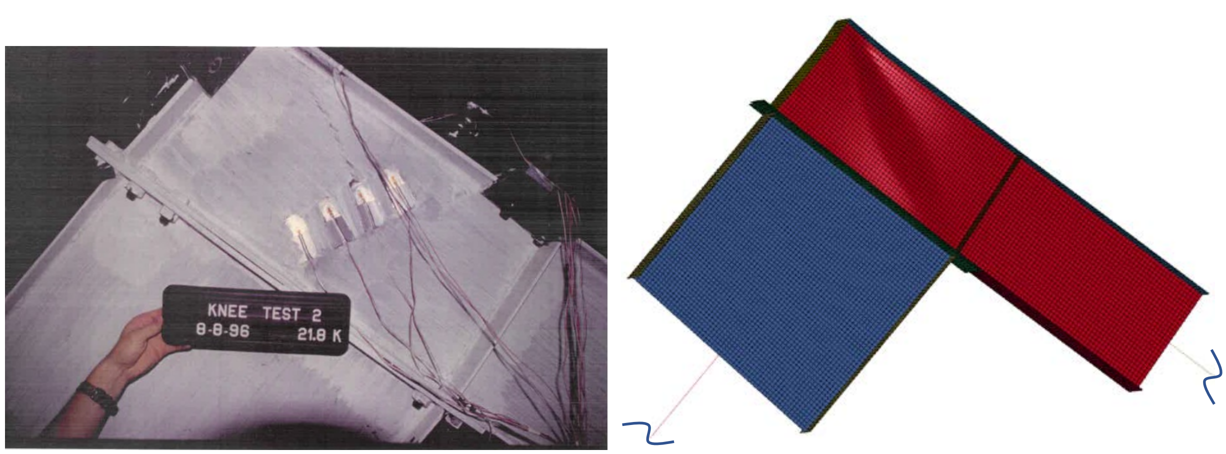

Figure 4b: Comparison of analytically obtained and experimentally observed deformation patterns, for validation analyses of the knee joint Specimen 2 tested by Young and Murray (1997)

4. Parametric Study and Validation of the Theoretical Model

The panel strength obtained with the proposed theoretical model primarily depends on three dimensionless variables, namely, panel web slenderness, $\max(h_c, h_r)/t_w$, panel web aspect ratio, h_r/h_c , and the panel flange flexural strength parameter, M_P^* . The range for the values of these variables in the 56 prototype structures has been determined based on the responses of an industry survey and is given in Table 2. More information about the industry survey can be found in Wei et al. (2017). A detailed description of the dimensions of the prototype structures is also provided in Table 5 of the Appendix. In all prototype structures considered, the parameter M_P^* is identical for both flanges at the corner edges of the panel zone (i.e. the flanges on the two outside edges of the knee joint are assumed identical). All prototype configurations have a roof slope of 2:12 and a vertical end-plate connection. No stiffener is used across the panel zone.

Table 2 Values and combinations of the three variables for the design of prototype structures

$\max(h_c, h_r)/t_w$	h_r/h_c	M_P^*
144, 192, 256, 292	0.67, 1.50	0.010
	0.75, 1.00, 1.33	0.005, 0.010, 0.050, 0.100

The validated modeling scheme was used to create 56 models for the prototype knee joint configurations. The maximum applied displacement in the models was equal to 10 inches (corresponding to a story drift of approximately 4% ~ 5% for most of the configurations).

The analyses of the prototype structures yielded two types of force-displacement behavior in terms of post-yielding response. The first type corresponds to softening, where the strength degraded after reaching a peak capacity at a relatively low level of deformation, as shown in Fig. 5a. Softening was associated with kinks (i.e. large rotations) forming in the exterior flanges at the location of the flange plastic hinges. The second type is shown in Fig. 5b and corresponds to hardening, where an initial, linear segment of the load-displacement curve reaches a threshold value of force, after which point the force-displacement curve retains a positive, hardening slope. Softening occurred for cases with M_P^*, equal to 0.005 or 0.01, where the flanges on the outside of the panel zone were weaker and experienced large inelastic deformations. Conversely, hardening response was obtained for higher values of M_P^*, corresponding to cases with less deformable

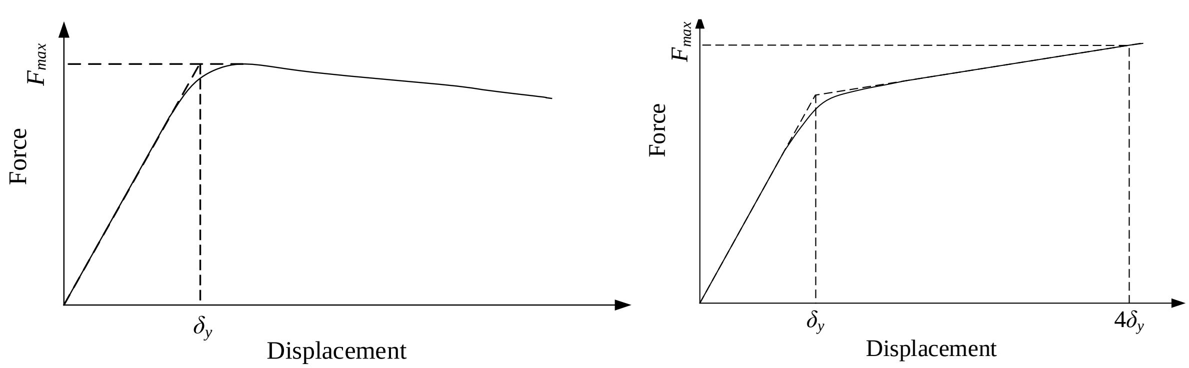

(a) Softening (b) Hardening

Figure 5: Different types of force-displacement curves obtained in analyses of prototype structures and definition of peak force, F_{max}

flanges, which are adequately stiff to anchor the tension field action and allow the development of post-buckling strength in the panel zones, associated with hardening in the elastoplastic material. Given that the applied force in the load-deformation curve is always increasing, a definition of the obtained shear strength is necessary. The present study defines the peak force for hardening response as the force corresponding to a displacement value equal to four times the yield displacement, as shown in Fig. 5b. This approach was originally employed by Krawinkler (1978) to define the ultimate shear strength of panel zones.

After the maximum applied force is obtained from the load-deformation curve, the maximum moment M_u and axial force P_u applied at the rafter face of the panel zone can be determined, based on the geometry of the knee joint. The panel shear strength from the FEA results, V_{FEA}, is calculated using the following equation:

$$V_{FEA} = \frac{1}{1.08}\left(\frac{M_u}{h_{ro}} - \frac{P_u}{2}\right) \tag{16}$$

where h_{ro} is the distance between the center lines of the rafter flanges at the rafter face of the panel zone. The "1.08" factor in Eq (16) is equal to the average ratio of analytically obtained over experimentally recorded shear strength values in the validation analyses of Section 3. For this reason, the same factor is used to correct the shear strength values obtained in the parametric analyses.

A modification to the prediction equation is calibrated to account for the idealized assumptions made during the formulation of the theoretical model, e.g., that the panel web plate is simply supported in the out-of-plane direction and rigidly anchored to resist in-plane deformation at the edges connected to the column and rafter, that the stress distribution across the tension field strip is uniform, and that the geometry of the panel zone is a rectangle as well. Specifically, the shear buckling coefficient, C_v, is modified to account for the limited accuracy of these idealized assumptions. A modification with a first-order linear equation is made to C_v as follows:

$$C_v^* = C_1 C_v + C_2 \tag{17}$$

where C_1 and C_2 are constant coefficients determined by solving an optimization problem, aimed to minimize the root mean square (RMS) of the values, ($V_{PZ}/V_{FEA} - 1$). A Generalized Reduced Gradient (GRG) nonlinear solving method (Lasdon et al. 1978) is adopted for the solution of the optimization problem, and the optimal values of C_1 and C_2 were found to be equal to 0.50 and 0.17, respectively.

Table 5 in the Appendix summarizes the results for the 56 models from the FEA compared to those calculated with the modified theoretical model. Additional details are included in Wei et al. (2017). The modified equations were found to produce panel zone shear strength that were satisfactorily close to the shear strength from the FEA models by 1% on average with a standard deviation of 4% for the difference, and the difference is less than 10% for all the cases. The accuracy of the modified theoretical equations is also reflected in Fig. 6, which presents the relation between the panel shear strength from the FEA and the theoretical equations.

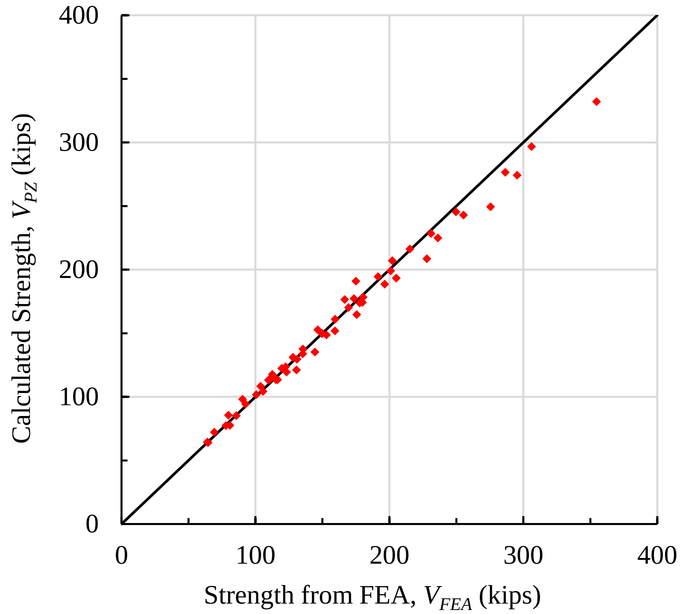

Figure 6: Evaluating panel zone shear strength equations as compared to FEA results

Table 3 shows the comparison of shear strength from tests and from the theoretical model for two test specimens (Young and Murray 1997). The predicted shear strength from the modified equations agrees reasonably well with test results.

Table 3 Validation of Theoretical Model against Test Data

Specimen #	V_{exp} (kips)	V_{PZ} (kips)	V_{PZ}/V_{exp}
1	43.2	43.5	101%
2	46.8	43.6	93%

Table 4 Summary of the Computational Study

Total number of models	98
Panel web thickness (in)	0.164 – 0.250
Panel web height (in)	24 – 48
Panel web width (in)	24 – 48
Panel flange width (in)	5 – 16
Panel flange thickness (in)	0.25 – 1.5
Panel web slenderness max(h_c, h_r)/t_w	144 – 292
Panel web aspect ratio h_r/h_c	0.67 – 1.50
Panel flange flexural strength parameter M_{P1}^*	0.005 – 0.1
Panel flange flexural strength parameter M_{P2}^*	0.005 – 0.1
Colum and rafter sectional property	Prismatic, tapered
Orientation of end-plate connection	Vertical, horizontal, sloped
Roof slope	0:12, 2:12, 4:12
Average of V_{PZ}/V_{FEA}	99%
Standard deviation of V_{PZ}/V_{FEA}	4%
Percentage of models with 15% difference or less	100%
Percentage of models with 10% difference or less	98%

Additional studies involving 42 prototype structures were also conducted to investigate the impact of several other variables on the knee joint panel zone shear resistance, such as column and rafter lengths, use of tapered sections, different dimensions for the two exterior flanges of the panel, orientation of end-plate connection, and roof slope. Table 4 provides a summary of the results for all the prototype knee joint configurations. For the range of parameter values considered in this study, the modified prediction equations of the theoretical model can accurately predict the panel zone shear strength.

5. Conclusions and Recommendations

This study used plastic analysis to formulate a theoretical model which predicts the post-buckling shear strength of knee joint panel zones subjected to positive bending (bottom flange of rafter in tension) including partially developed tension field action. The panel shear strength was found to primarily depend on three design parameters, namely, flange flexural strength, panel aspect ratio, and panel slenderness. A parametric computational study involving 56 models with a range of values for the three parameters was conducted to validate and fine-tune the proposed equations. Additional studies were also performed to investigate the application of the proposed equations for predicting shear strength of knee joint configurations with different member lengths, different section types (prismatic or tapered), different flexural strength for the two exterior panel flanges, different orientations of end-plate connections, and different values of roof slope.

For the range of parameters considered in this study, the modified equations can accurately predict the panel shear strength. However, there are three reasons to be cautious with configurations that produce softening response including: 1) the cumulative plastic strains were larger than the models with hardening behavior and thus softening joints may be more prone to fracture, 2) the panel zone shear strength is expected to be more sensitive to initial imperfections and residual stresses, and 3) the consequences of reaching this limit state are worse because it is a brittle failure mode. Therefore, the use of TFA in positive bending is not recommended for design of configurations that will produce softening (normalized flange flexural strength less than 0.05), until further testing is conducted.

The proposed equations for panel zone shear strength, V_{PZ}, in knee joints with $M_P^* \geq 0.05$ subjected to positive bending are summarized below:

$$V_{PZ} = V_{cr} + V_{TFA} \tag{18}$$

where
$$V_{cr} = A_v \tau_{cr} = d_c t_w C_v^* \sigma_{yw} \Big/ \sqrt{3} \tag{19}$$

$$V_{TFA} = \left[\frac{M_{P1}^* - M_{P2}^* - M_{P,min}^*}{6\,tan\,\theta} + cos\,\theta \sqrt{\frac{C_t}{3}} \left(\sqrt{M_{P1}^* + M_{P,min}^*} + \sqrt{M_{P2}^* + M_{P,min}^*} \right) \right] h_c t_w \sigma_{yw} \tag{20}$$

$$C_v^* = \frac{\sqrt{3}}{2} K \left[\frac{\pi^2\, E \big/ \sigma_{yw}}{12\left(1-\mu^2\right)} \right] \left(\frac{t_w}{h_c} \right)^2 + 0.17 \tag{21}$$

$$K = \begin{cases} 5.34 + 4\left(\dfrac{h_c}{h_r}\right)^2 & \text{for } \dfrac{h_c}{h_r} < 1.0 \\ 5.34\left(\dfrac{h_c}{h_r}\right)^2 + 4 & \text{for } \dfrac{h_c}{h_r} > 1.0 \end{cases} \tag{22}$$

$$C_t = -\frac{\sqrt{3}C_v^* \, sin\, 2\theta}{2} + \sqrt{1 + \frac{\left(C_v^*\right)^2}{3}\left(\left(\frac{3\, sin\, 2\theta}{2}\right)^2 - 3\right)} \tag{23}$$

$$\theta = arctan\frac{h_r}{h_c} \tag{24}$$

$$M_{P1}^* = \frac{M_{P1}}{M_y} = \frac{3b_{f1}t_{f1}^2\sigma_{yf}}{2t_w h_c^2 \sigma_{yw}} \tag{25}$$

$$M_{P2}^* = \frac{M_{P2}}{M_y} = \frac{3b_{f2}t_{f2}^2\sigma_{yf}}{2t_w h_c^2 \sigma_{yw}} \tag{26}$$

$$M_{P,min}^* = min\left(M_{P1}^*, M_{P2}^*\right) \tag{27}$$

The work described in this paper is based on using finite element analyses to extrapolate from the results of two experimental tests (Young and Murray 1997). The FEA models are not capable of capturing fracture which could limit the panel zone shear strength, nor do they address detailing requirements (e.g. stronger welds around the panel zone) that might be needed to reach the panel zone shear strengths given by the proposed equations. For this reason, large-scale experimental tests are deemed necessary to further validate the proposed design approach.

Acknowledgments
This work was supported by the Metal Building Manufacturers Association (MBMA). Dean Jorgenson, President of Metal Building Software, Inc. provided the design of some prototype metal building gable frames. Several metal building manufacturers provided valuable feedback on the industry survey mentioned in Section 4. Thanks to the MBMA advisory group for their input. The Advanced Research Computing (ARC) at Virginia Tech provided high-performance computing resources which facilitated the finite element study. Any opinions expressed in this paper are those of the authors alone, and do not necessarily reflect the views of MBMA.

References

American Institute of Steel Construction. (2016). *Steel construction manual* (15th ed.). Chicago, Illinois: American Institute of Steel Construction.

Hughes, T. J., & Liu, W. K. (1981). Nonlinear finite element analysis of shells: Part I. Three-dimensional shells. *Computer methods in applied mechanics and engineering*, *26*(3), 331-362.

Krawinkler, H. (1978). Shear in beam-column joints in seismic design of steel frames. *Engineering Journal*, *15*(3).
Lasdon, L. S., Waren, A. D., Jain, A., & Ratner, M. (1978). Design and testing of a generalized reduced gradient code for nonlinear programming. *ACM Transactions on Mathematical Software (TOMS)*, *4*(1), 34-50.
Livermore Software Technology Corporation. (2016a). *LS-DYNA Keyword User's Manual: Volumn I* (Version R9.0). Livermore, CA.: Livermore Software Technology Corporation.
Livermore Software Technology Corporation. (2016b). *LS-DYNA Keyword User's Manual: Volumn II* (Version R9.0). Livermore, CA.: Livermore Software Technology Corporation.
Metal Building Manufacturers Association. (2012). *Metal Building Systems Manual.* Cleveland, Ohio: Metal Building Manufacturers Association.
Murray, T. M., & Shoemaker, W. L. (2002). *Flush and extended multiple-row moment end-plate Connections*. American Institute of Steel Construction.
Porter, D. M., Rockey, K. C., & Evans, H. R. (1975). Collapse Behaviour of Plate Girders Loaded in Shear. *Structural Engineer, 53*(8), 313-325.
Rockey, K. C., & Skaloud, M. (1972). Ultimate load behaviour of plate girders loaded in shear. *Structural Engineer, 50*(1), 29-47.
Timoshenko, S. P., & Gere, J. M. (1961). Theory of elastic stability. 1961. *McGrawHill-Kogakusha Ltd, Tokyo*, 9-16.
Wei, G., Koutromanos, I., Murray, T. M., & Eatherton, M. R. (2017). *Computational Study of Tension Field Action in Gable Frame Panel Zones* (Rep. No. CE/VPI-ST-17/03). Blacksburg, Virginia: Virginia Tech.
Young, J., & Murray, T. M. (1997). *Experimental Investigation of Positive Bending Moment Strength of Rigid Knee Connections* (Rep. No. CE/VPI-ST 97/08). Blacksburg, Virginia: Virginia Tech.
Ziemian, R.D. (ed.) (2010), *Guide to Stability Design Criteria for Metal Structures*, 6th Ed., John Wiley & Sons, Inc., Hoboken, NJ.

Appendix

Table 5 Comparison of results from FEA and the modified theoretical equations

Model #	t_w (in)	h_c (in)	h_r (in)	b_f (in)	t_f (in)	t_p (in)	l_c (ft)	l_r (ft)	V_{FEA} (kips)	V_{PZ} (kips)	$\frac{V_{PZ}}{V_{FEM}}$
1	0.2500	36	24	6	0.625	0.875	15	18.5	189	191	109%
2	0.2500	36	27	8	0.375	0.750	15	17.0	172	161	101%
3	0.2500	36	27	6	0.625	0.875	15	19.5	180	177	106%
4	0.2500	36	27	10	1.000	1.125	15	29.5	250	228	99%
5	0.2500	36	27	14	1.250	1.250	15	38.5	319	274	93%
6	0.2500	36	36	8	0.375	0.750	15	20.5	156	135	94%
7	0.2500	36	36	6	0.625	0.875	15	23.0	162	150	100%
8	0.2500	36	36	10	1.000	1.125	15	34.5	217	199	99%
9	0.2500	36	36	14	1.250	1.250	15	45.0	276	243	95%
10	0.2500	27	36	6	0.313	0.750	15	18.5	126	113	97%
11	0.2500	27	36	9	0.375	0.750	15	21.5	129	122	102%
12	0.2500	27	36	10	0.750	1.000	15	31.0	158	153	104%
13	0.2500	27	36	12	1.000	1.125	15	38.0	195	178	99%
14	0.2500	24	36	6	0.375	0.750	15	20.5	120	114	103%
15	0.2500	48	32	10	0.625	0.875	15	26.0	218	207	102%
16	0.2500	48	36	8	0.500	0.875	15	23.0	194	174	97%
17	0.2500	48	36	10	0.625	0.875	15	27.5	207	194	102%
18	0.2500	48	36	12	1.250	1.250	15	41.5	309	277	97%
19	0.2500	48	36	16	1.500	1.375	15	52.5	383	332	94%
20	0.2500	48	48	8	0.500	0.875	15	27.5	172	152	95%
21	0.2500	48	48	10	0.625	0.875	15	33.0	183	170	100%
22	0.2500	48	48	12	1.250	1.250	15	49.5	270	245	98%

Table 5 (Continued) Comparison of results from FEA and the modified theoretical equations

Model #	t_w (in)	h_c (in)	h_r (in)	b_f (in)	t_f (in)	t_p (in)	l_c (ft)	l_r (ft)	V_{FEA} (kips)	V_{PZ} (kips)	$\frac{V_{PZ}}{V_{FEM}}$
23	0.2500	48	48	16	1.500	1.375	15	62.5	331	297	97%
24	0.2500	36	48	8	0.375	0.750	15	24.5	141	121	93%
25	0.2500	36	48	6	0.625	0.875	15	27.5	146	134	99%
26	0.2500	36	48	10	1.000	1.125	15	41.0	187	177	102%
27	0.2500	36	48	14	1.250	1.250	15	53.5	233	216	100%
28	0.2500	32	48	6	0.500	0.875	15	26.0	133	120	97%
29	0.1875	48	32	8	0.625	0.875	15	22.5	146	138	102%
30	0.1875	48	36	6	0.500	0.750	15	19.5	124	113	98%
31	0.1875	48	36	8	0.625	0.875	15	24.0	138	131	102%
32	0.1875	48	36	14	1.000	1.125	15	39.5	222	193	94%
33	0.1875	48	36	14	1.500	1.375	15	48.5	298	249	91%
34	0.1875	48	48	6	0.500	0.750	15	22.5	109	102	101%
35	0.1875	48	48	8	0.625	0.875	15	28.0	122	118	104%
36	0.1875	48	48	14	1.000	1.125	15	46.5	192	174	98%
37	0.1875	48	48	14	1.500	1.375	15	57.5	255	225	95%
38	0.1875	36	48	6	0.375	0.750	15	21.0	87.5	77.6	96%
39	0.1875	36	48	6	0.500	0.750	15	23.0	92.6	85.1	99%
40	0.1875	36	48	8	1.000	1.000	15	35.5	132	124	101%
41	0.1875	36	48	10	1.250	1.125	15	44.0	162	150	100%
42	0.1875	32	48	9	0.375	0.625	15	23.0	84.3	77.3	99%
43	0.1644	48	32	10	0.500	0.750	15	21.5	119	113	103%
44	0.1644	48	36	9	0.375	0.625	15	18.5	100	94.3	102%
45	0.1644	48	36	10	0.500	0.750	15	23.0	112	108	104%
46	0.1644	48	36	12	1.000	1.125	15	36.0	190	165	94%
47	0.1644	48	36	16	1.250	1.250	15	47.0	246	209	91%
48	0.1644	48	48	9	0.375	0.625	15	21.0	86.3	85.5	107%
49	0.1644	48	48	10	0.500	0.750	15	26.5	97.6	98.0	108%
50	0.1644	48	48	12	1.000	1.125	15	42.5	165	149	97%
51	0.1644	48	48	16	1.250	1.250	15	55.5	212	188	96%
52	0.1644	36	48	5	0.375	0.625	15	18.5	69.9	64.0	99%
53	0.1644	36	48	10	0.375	0.625	15	22.0	74.9	72.1	104%
54	0.1644	36	48	12	0.750	1.000	15	37.0	114	104	99%
55	0.1644	36	48	14	1.000	1.125	15	46.5	141	130	99%
56	0.1644	32	48	8	0.375	0.625	15	21.5	69.2	64.4	100%
										Average:	99%
										Standard deviation:	4%